Ultracold strontium clock: Applications to the measurement of fundamental constant variations

A.D. Ludlow[a], S. Blatt, T. Zelevinsky[†], G.K. Campbell, M.J. Martin, J.W. Thomsen[‡],
M.M. Boyd, and J. Ye

JILA, National Institute of Standards and Technology and University of Colorado 440 UCB,
Boulder, CO 80309-0440, USA

Abstract. We describe the application of high accuracy Sr spectroscopy to the measurement of the variation of the fundamental constants of nature. We first describe recent progress of the JILA Sr optical frequency standard, with a systematic uncertainty evaluation at the 10^{-16} fractional frequency level. Using recent internationally based measurements of the Sr clock frequency, we show improved constraints of gravitational and temporal changes in the fine structure constant and the electron-proton mass ratio. Finally, we describe how ultracold atomic strontium, confined in an optical lattice, can be associated into molecular dimers and be used for a model-independent measurement of the variation of the electron-proton mass ratio.

1 Introduction

Atomic clocks are one of several vital tools which help to determine how the fundamental constants, as some theories predict, couple to the universe [1,2]. They complement astronomical and other measurements intended to sample a large fraction of the history of the universe [3,4]. The clocks' ability to make meaningful contributions to this field stems from their unmatched measurement accuracy and precision. The atomic and molecular transitions at the heart of these standards naturally depend on the values of key fundamental constants such as the fine structure constant, the electron-proton mass ratio, and the light quark masses. As these clocks continue to advance in measurement precision and accuracy, their ability to constrain fluctuations of these constants grows. This is particularly true for optical frequency standards, which now outperform the best Cs microwave standards [5,6]. Here we report on the progress of the Sr optical frequency standard based on fermionic strontium confined in an optical lattice. By careful design and characterization, this standard now exhibits uncertainty at the 10^{-16} fractional frequency level. We demonstrate km-scale remote comparison of the Sr standard to other optical and microwave standards, a useful tool for multi-species measurements which will provide further valuable data for fundamental constant measurement.

The Sr clock transition has very weak dependence on changes in the fine structure constant [7]. While this limits the magnification of fundamental constant variation, it makes Sr very well suited as a measurement anchor. Frequency standards based on species with very high sensitivity may utilize Sr as a stable reference, making data interpretation more straightforward. Recent high accuracy measurements of the Sr clock transition frequency versus Cs by three groups worldwide show excellent agreement [8–13], making the Sr clock transition the best

[a] e-mail: `ludlow@jila.colorado.edu`

[†] *Present address*: Columbia University, Dept. of Physics, New York, NY, USA.

[‡] *Permanent address*: The Niels Bohr Institute, Universitetsparken 5, 2100 Copenhagen, Denmark.

agreed upon optical transition frequency. This enables analysis of the combined measurement data set of all three groups for clock frequency changes resulting from the potential change in fundamental constants.

Sr has also shown strong potential for the measurement of interatomic effects [14–17], including molecular association. Ultracold atomic strontium can be efficiently associated into an ultracold gas of Sr_2 [15]. Since the vibrational energy intervals of the Sr dimer are sensitive to the electron-proton mass ratio, the high precision atomic spectroscopy exhibited in the Sr optical frequency standard can be applied to Sr dimer spectroscopy in an optical lattice, allowing a clean, model-independent measure of changes in the electron-proton mass ratio at the 10^{-15}/yr fractional level [14].

2 The Sr optical frequency standard

For more than half a century, frequency standards based on atomic and molecular transitions have proven to be the most stable and well-defined frequency sources. During most of this history, Cs-based microwave standards have demonstrated the highest performance. Because of this, for more than 40 years, the SI second has been defined by reference to the Cs clock transition at 9.2 GHz. State-of-the-art Cs standards, based on laser cooled cesium in an atomic fountain, now demonstrate fractional frequency uncertainty below 1×10^{-15} [5,6]. More recently, frequency standards based on optical transitions (e. g. [10,12,17–21]) are demonstrating performance approaching the best Cs standards, in terms of both the frequency instability and uncertainty. These standards enjoy the fact that their base operational frequency is in the optical domain, meaning that frequency shifts and measurement noise of the atomic transition typically contribute fractionally smaller to the large optical frequency. Already more stable than their microwave counterparts, these optical systems continue to promise the potential for substantial improvements in their frequency uncertainty. Indeed, results outperforming the best Cs fountains are already being reported [17,18,22].

Optical standards have naturally been categorized into two types: those based on a single trapped ion, and those based on a large ensemble of neutral atoms. Regardless of this distinction, all good optical standards share a set of key characteristics. The most critical is the existence of a conveniently accessed optical transition which is well-defined (narrow linewidth) and insensitive to environment-induced frequency shifts. For the case of strontium, this is naturally found in the fermionic isotope, ^{87}Sr (see Figure 1). A very weak transition exists from the ground state $5s^2\ ^1S_0$ to the first excited state $5s5p\ ^3P_0$. A dipole transition between these two states violates multiple selection rules, but here is only weakly allowed due to hyperfine mixing of the $^3P_0$ state with the nearby $^3P_1$ and the higher lying $^1P_1$ state. This clock transition has a natural linewidth less than 2 mHz [23], offering the potential for exceptionally long coherent laser-atom interaction times during spectroscopy. With $J = 0$ for both states, $^1S_0$ and $^3P_0$ remain insensitive to a number of environmental effects [24]. Both states have only a weak Zeeman shift coefficient originating from the nuclear spin $I = 9/2$ and the relative shift coefficient between the states is even smaller [23].

Beyond the well-suited clock transition, other Sr transitions facilitate the atomic manipulation used to prepare strontium for use as a frequency standard. The strong $^1S_0$-$^1P_1$ transition (wavelength = 461 nm, linewidth = 32 MHz) is a mostly closed $J = 0 - J = 1$ transition excellent for laser cooling strontium from a thermal source. Doing so collects millions of cold Sr atoms at mK temperatures in a magneto-optical trap (MOT). Spectroscopy of the optical clock transition benefits from even colder Sr samples, and the $^1S_0$-$^3P_1$ transition provides relatively convenient means to further laser cool ^{87}Sr to below μK temperatures [25,26]. From this standpoint, ^{87}Sr enjoys several dipole transitions, each in a different regime of transition strength and all of which facilitate its use for an optical frequency standard.

Interrogation of any atomic transition must confront the issue of atomic motion. For free space interrogation of an atomic transition, the Doppler effect can lead to dramatic broadening and shift mechanisms which degrade the suitability of the atom for precise frequency referencing. One approach to overcome this effect has been trapping a single ion in a confining electric
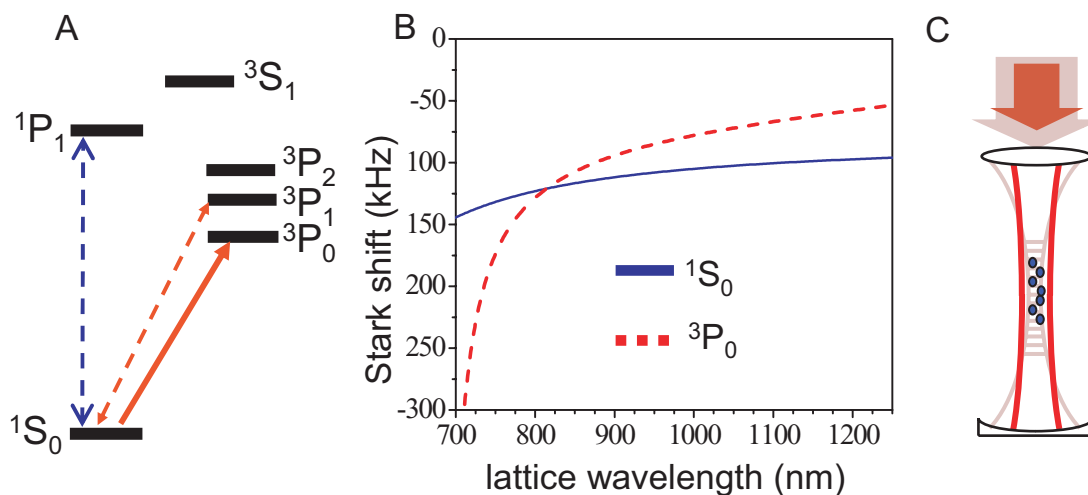
Fig. 1. A) Strontium energy level diagram. The blue dashed arrow denotes the $^1S_0$-$^1P_1$ laser cooling transition, the red dashed arrow the $^1S_0$-$^3P_1$ narrow line laser cooling transition, and the solid red arrow the $^1S_0$-$^3P_0$ clock transition. B) The AC Stark shift induced by the lattice laser on the clock states (laser intensity $I \simeq 5\,\mathrm{kW/cm^2}$). At the point near $\lambda = 800\,\mathrm{nm}$, the Stark shifts are matched giving no net shift for the clock transition. C) Schematic of the 1-D standing wave optical lattice, with the Sr atoms trapped at the focal point. The clock probing laser (small arrow) is co-propogated and co-polarized with the lattice laser (large arrow).

field. Doing so exploits the ion charge as a handle for confinement, but the field has minimal perturbation on the internal clock states. While neutral atom standards have made substantial progress with free space interrogation [27,28], Doppler effects require very careful control and can be a prohibitive complexity. In the last few years, atomic confinement of a large neutral atom ensemble has been explored extensively [8,9,29]. Here, in order to provide atomic confinement, the clock states are strongly perturbed by applying an intense light field. This light field both induces an atomic dipole moment as well as interacts with the induced dipole to trap the atom. In order to prevent clock transition shifts resulting from this perturbation, the light field is designed to perturb the two clock states identically, such that no net shift between the states is present. For Sr, this is illustrated in Fig. 1, where the AC Stark shift induced by the confining light field is matched for $^1S_0$ and $^3P_0$ when the light field wavelength is at the so-called magic wavelength $\lambda \simeq 813\,\mathrm{nm}$. As shown in Fig. 1, we typically trap the strontium in a standing wave 1-D optical lattice and probe the atoms along the strong confinement axis where they reside in the Lamb-Dicke and resolved-sideband regime [30]. Similar work is being explored in ytterbium [21] and mercury [31]. In the case of Sr, measurement of the clock transition now reaches an accuracy rivaling the best Cs standards. This atomic confinement is similar in spirit to the trapped ion case, but additionally enjoys large atom number, which facilitates higher signal-to-noise ratios of the atomic transition measurement.

To exploit the high frequency resolution afforded by a narrow clock transition, it is crucial to probe the atom with a stable, coherent optical wave. This requirement marries the optical frequency standard with state-of-the-art techniques for laser stabilization. Laser light is typically frequency and phase stabilized to a passive Fabry-Perot optical cavity. Using Pound-Drever-Hall stabilization [32], the laser frequency is tightly locked to a resonance of the cavity, defined by the cavity optical length. The resulting laser stability is thus determined by the cavity length stability. By designing the cavity to be robust against length changes as well as isolating the cavity from noise sources which compromise the length stability, a free-running laser with MHz linewidth can be made to have sub-Hz linewidth. For the strontium system, a diode laser at 698 nm is locked to a high finesse ($F = 250,000$) optical cavity. The optical cavity is mounted in a symmetric fashion which reduces cavity length sensitivity to elastic deformations of the cavity originating from vibrations [33]. By making an optical heterodyne beat measurement
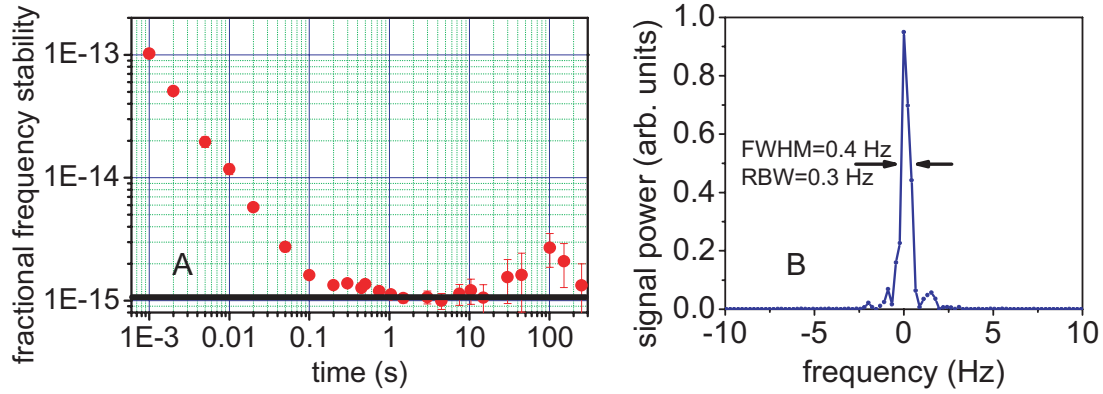
Fig. 2. Performance characteristics of one cavity stabilized clock laser obtained by heterodyne beating two similar, but independent, laser systems. A) The frequency stability of the laser (expressed as a fraction of the laser frequency) as a function of time. The thick black line denotes the theoretically estimated laser instability due to the thermal mechanical noise of the cavity. B) Measurement of the sub-Hz laser linewidth.
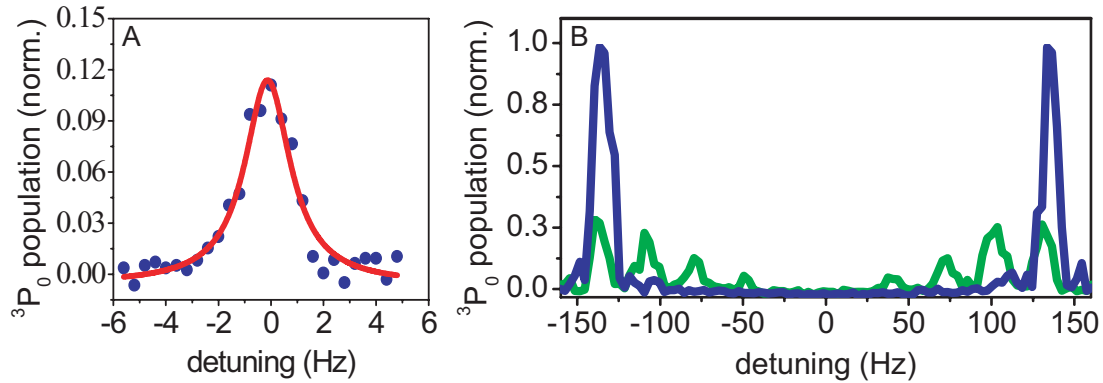

Fig. 3. A) The ultranarrow Sr clock transition, with an experimentally observed 2 Hz linewidth. This line, taken with a laser probe time of 480 ms duration, is a single π-transition from the $m_F = 5/2$ nuclear spin state in the presence of a bias magnetic field. B) Green: spectra of all the π-transitions under a bias magnetic field with a laser probing time of 80 ms. Blue: Same spectra, but with state preparation to the $m_F = \pm 9/2$ nuclear spin states. The vertical axes in A and B are normalized to the peak amplitude of the doubly spin-polarized $m_F = \pm 9/2$ transition.

between two similar laser systems, the stabilized laser linewidth is measured to be sub-Hz (see Fig. 2) [34]. The laser instability, expressed as the fractional Allan deviation, is also shown, and is 10^{-15} between 100 ms and 100 s. The limit to the laser instability is thermal mechanical noise of the mirror substrates [35]: thermal energy off-resonantly excites vibrational modes of the mirror substrate and dielectric coating layers, leading to Brownian motion of the mirror surface and reducing the cavity length stability.

The narrow linewidth laser source is then used to interrogate the clock transition. The optical coherence from the laser source combined with the clean, uniform atomic confinement provided for the clock states by the optical lattice make for the possibility of long coherent atom-laser interaction times. Clock transition interrogation of up to 480 ms yields atomic spectra as narrow as that shown in Fig. 3 [36]. The 2 Hz linewidth is consistent with the Fourier limit, and represents a line quality factor of $Q \geq 2 \times 10^{14}$, the highest observed Q for coherent spectroscopy. This frequency resolving power of narrow atomic spectra plays a key role in enabling the Sr measurement precision. As a key ingredient to this precision, the fractional
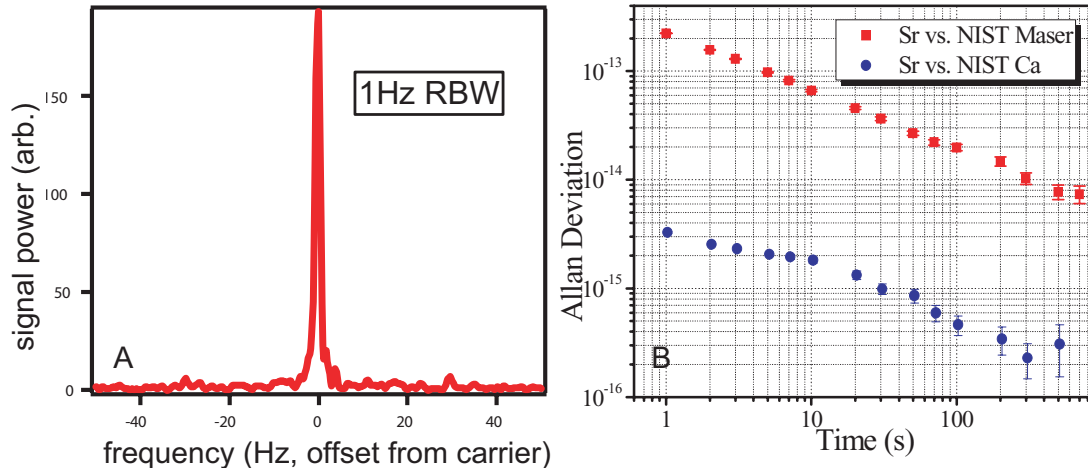
Fig. 4. (A) Optical laser linewidth measurement made across the 4 km fiber link. The JILA frequency comb was locked to the Sr clock laser, and a Nd:YAG was locked to the comb and transferred to NIST with fiber phase noise cancellation. The measurement was taken at NIST by making a heterodyne beat of the transferred Nd:YAG light with a NIST frequency comb locked to the Hg$^+$ ion clock laser. The resulting linewidth is 1 Hz. (B) Red squares: The fractional instability for a measurement between the JILA Sr standard and the NIST Cs-calibrated H-maser. Blue circles: The fractional instability between the JILA Sr standard and the NIST Ca standard.

instability of a frequency standard utilizing a transition with frequency ν and linewidth $\delta\nu$ can be expressed as:

$$\sigma_y\left(\tau\right) = \frac{\delta\nu}{\nu} \frac{\eta}{S/N\sqrt{\tau}} \tag{1}$$

Here S/N indicates the signal to noise ratio of the atomic transition measurement (rms, 1 Hz BW), τ is the averaging time, and η is a parameter close to unity whose exact values depend on details of the spectroscopic lineshape. The spectrum shown in Fig. 3, taken without any averaging (total measurement time is about 1 s per spectral point), reveals the capacity for an instability of 10^{-15} at 1 s.

When operated as a frequency standard, the clock states are probed by the stable laser and normalized excitation is detected. This excitation signal is used to feedback control the laser frequency to the atomic transition with a low bandwidth servo [17]. To exploit the stability of this optical standard, frequency measurements are ideally made with another optical standard. To accomplish this, we use an optical carrier transfer scheme over a fiber link (4 km) [37] to enable measurements with other optical standards located at the National Institute of Standards and Technology (NIST) Boulder campus [18, 21, 22, 38]. This transfer scheme uses round trip fiber phase noise cancellation which has been independently characterized, revealing that extra noise accumulated over the link leads to an instability between the transferred and the original frequency signal below 10^{-17} for all measured times longer than 1 s [37]. This is done by phase locking an octave-spanning, optical frequency comb to the Sr clock laser. A transfer laser operating at 1064 nm is then phase locked to the frequency comb, transferring the Sr standard stability and accuracy. The phase-noise-cancelled 1064 light arriving at NIST is then measured against a second frequency comb, which itself is phase locked to one of the NIST optical standards. Fig. 4 shows the effectiveness of this comparison scheme. Fig. 4(A) shows a 1 Hz optical linewidth measured between the transferred 1064 nm light and the NIST frequency comb locked to the Hg$^+$ clock laser, indicating the ability to transfer phase coherence across the optical spectrum and across long distances. Fig. 4(B) shows the measured instability, as given by the Allan deviation, between the Sr standard at JILA and the Ca standard at NIST. At 1 s the instability is several 10^{-15}, averaging down to a few 10^{-16} at several hundred seconds.

We have conducted an evaluation of systematic shifts of the Sr optical frequency by measurement with the NIST Ca standard. In order to reduce the clock transition sensitivity to

Table 1. Systematic frequency shifts and their uncertainties for the ^{87}Sr frequency standard.

Contributor	Correction (10^{-16})	Uncertainty (10^{-16})
Lattice Stark (scalar/tensor)	−6.5	0.5
Hyperpolarizability (lattice)	−0.2	0.2
BBR Stark	52.1	1.0
AC Stark (probe)	0.2	0.1
1st order Zeeman	0.2	0.2
2nd order Zeeman	0.2	0.02
Density	8.9	0.8
Line pulling	0	0.2
Servo error	0	0.5
2nd order Doppler	0	≪0.01
Systematic total	54.9	1.5

1st-order Zeeman shifts, prior to spectroscopy we optically pump the mixed m_F populations of $^1S_0$ into $m_F = \pm 9/2$. An example of this optical pumping is shown in the spectrum of Fig. 3, measuring the π-transitions under a bias magnetic field to lift their degeneracy. Under a bias field during clock operation, the $\pm 9/2$ states are intermittently interrogated and the average of the two serves as the clock frequency. Since the two transitions have equal and opposite 1st-order Zeeman dependence, the average retains no dependence, while the 2nd-order Zeeman effect from the bias magnetic field leads to a relative shift of $\sim 10^{-17}$. The effect of the lattice laser on the atomic transition is studied to ensure operation close to λ_{magic}. Previous measurements indicate that at typical operating intensities, a one GHz deviation of the lattice laser from the "magic" operating point yields a 1 Hz clock transition shift [8]. To stabilize the lattice laser well below the MHz level, it is phase locked to the frequency comb which itself is locked to the Sr clock transition.

For the first time, we observe an atomic density dependent shift of the clock transition for these ^{87}Sr fermions. This shift depends on the excitation fraction as well as the nuclear spin state. During clock operation, control of these experimental parameters enables control of the density shift at the 10^{-16} level. Another critical systematic shift is the Stark shift induced by blackbody radiation. The uncertainty in this shift stems equally from the uncertainty in the static atomic polarizability (1%) [39] as well as temperature inhomogeneity of the vacuum chamber surrounding the lattice-trapped atoms. Each systematic shift, as well as the total shift with uncertainty of 1.5×10^{-16}, is summarized in Table 1. This characterization of the Sr standard enables high accuracy frequency measurements which can be applied to constraints on fundamental constant changes.

3 Constraints of fundamental constant variation using atomic Sr

With the systematic frequency shifts well characterized, a remaining issue is measurement of the absolute frequency of the Sr lattice clock relative to a Cs primary standard. At JILA, absolute frequency measurements are performed using a NIST H-maser that is calibrated by the Cs fountain [5]. The microwave reference is transferred from NIST to JILA using a stabilized optical fiber link [40], allowing direct clock comparison using a fs-comb. The statistical uncertainty in the Sr-maser comparison averages down as $2 - 3 \times 10^{-13} \tau^{-1/2}$, requiring long averaging times to reach the Sr uncertainty limit.

We have made a total of five absolute frequency measurements of the ^{87}Sr $^1S_0$-$^3P_0$ transition over the last few years. The last two measurements have resulted in measurement uncertainties at or below the 1 Hz level. The first of these two used an unpolarized sample at zero B-field, and was made over a consecutive 24 hour period to average down with the H-maser. The final uncertainty was 2.5×10^{-15} [11]. The second used a doubly-nuclear-spin-polarized sample similar to that described in the previous section, and was made over a consecutive 48 hour period. The final uncertainty was $< 9 \times 10^{-16}$, limited by the Cs/H-maser operation [13].
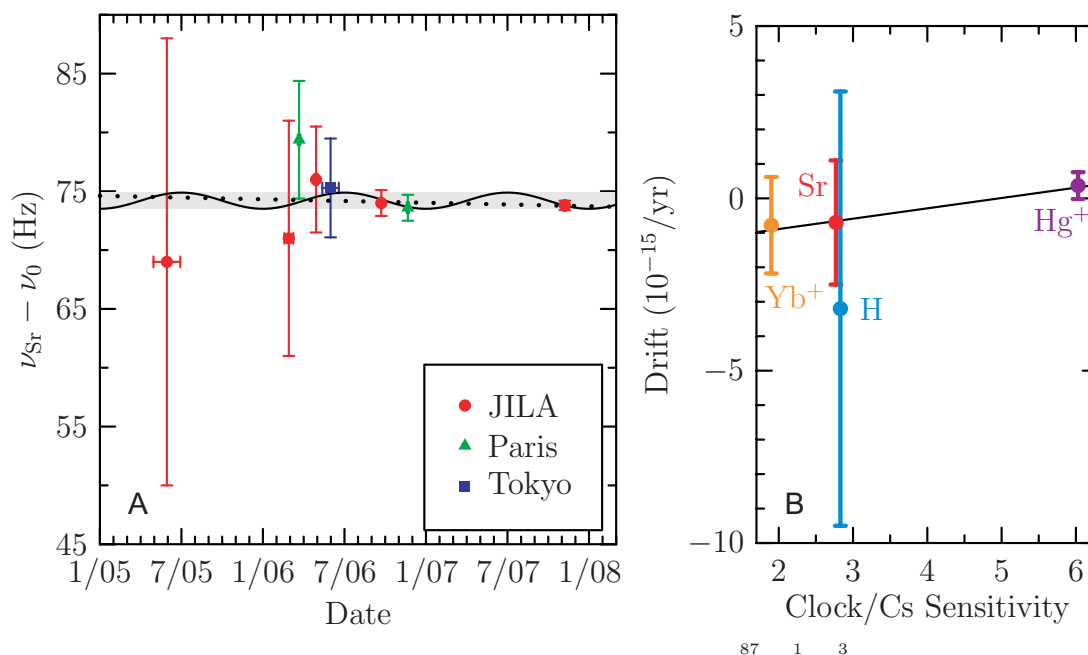
Fig. 5. (A) The combined absolute frequency measurements of the ^{87}Sr $^1S_0$-$^3P_0$ clock transition over the last few years. Red circles: JILA, Green triangles: Paris, Blue squares: Tokyo. The uncertainty along the date axis denotes the time interval over which the measurements were made. Frequency data is shown relative to $\nu_0 = 429\,228\,004\,229\,800$ Hz. A weighted linear (sinusoidal) fit to the data is denoted by the dotted (solid) line. The fit models are described in the text. (B) The combined absolute frequency measurement drift data for Yb$^+$, Hg$^+$, H, and Sr (plotted as a function of combined sensitivity). In this picture, the α drift is represented by the (negative of the) slope and the μ drift by the (negative of the) intercept point at zero sensitivity.

The Paris and Tokyo groups have also made high accuracy measurements of the Sr clock transition. The agreement between the different laboratories is near the 10^{-15} level, making Sr the most agreed upon optical frequency standard. Plotted against measurement date, the absolute frequency measurements of all 3 groups are shown in Fig. 5A (JILA: circles, Paris: triangles, Tokyo: squares).

Optical clock transitions exhibit dependence on the fine structure constant (α) through relativistic corrections to the transition frequency. The dependence is summarized by the sensitivity coefficient, K, which has been calculated for a variety of transitions in different atomic species (e.g. [2,7]). A change in α is related simply to a change in the transition frequency:

$$\frac{\delta\nu_{Sr}}{\nu_{Sr}} = K_{Sr}\frac{\delta\alpha}{\alpha}. \tag{2}$$

The Cs clock transition, based on hyperfine splitting, is additionally dependent on the electron-proton mass ratio $\mu = m_e/m_p$ [2,42]:

$$\frac{\delta\nu_{Cs}}{\nu_{Cs}} = (K_{Cs} + 2)\frac{\delta\alpha}{\alpha} + \frac{\delta\mu}{\mu}. \tag{3}$$

Here the total α sensitivity is given by $K_{Cs} + 2$. Since the Sr absolute frequency measurement is a ratio of the Sr frequency to the frequency definition provided by Cs, fluctuations in the absolute frequency measurement give the following dependence:

$$\frac{\delta(\nu_{Sr}/\nu_{Cs})}{\nu_{Sr}/\nu_{Cs}} = (K_{Sr} - K_{Cs} - 2)\frac{\delta\alpha}{\alpha} - \frac{\delta\mu}{\mu}. \tag{4}$$

$K_{Sr} = 0.06$ is much smaller than $K_{Cs} + 2 = 2.83$, and thus strontium serves as a frequency anchor to study α and μ dependence in Cs. Considering the special case of a linear drift of α and μ, the Sr absolute frequency measurements shown in Fig. 5 are fit to yield:

$$\frac{\delta(\nu_{Sr}/\nu_{Cs})}{\nu_{Sr}/\nu_{Cs}} = -1.0(1.8) \times 10^{-15}/\text{yr}. \tag{5}$$

Combined with absolute frequency measurements of optical transitions of other atomic species with different α sensitivity coefficients, K, the α and μ variation can be orthogonalized. Fig. 5(B) shows results of Hg$^+$, Yb$^+$, H, and Sr. The combined results give constraints of $\delta\alpha/\alpha = -3.3(3.0) \times 10^{-16}/\text{yr}$ and $\delta\mu/\mu = 1.6(1.7) \times 10^{-15}/\text{yr}$ [41]. Frequency measurements between Sr and other optical standards may be useful for investigations of α variations alone [22].

The Sr absolute frequency data can also be analyzed to look for coupling of α and μ values to the gravitational potential, as the earth's elliptical orbit brings the atomic frequency standards through the annually varying gravitational field from the sun. If the coupling of these constants is given by dimensionless parameters, k, the Sr frequency data can be fit with the following functional form:

$$\frac{\delta(\nu_{Sr}/\nu_{Cs})}{\nu_{Sr}/\nu_{Cs}} = [(K_{Cs} + 2 - K_{Sr})k_\alpha + k_\mu]\frac{Gm_{sun}}{ac^2}\epsilon\cos(\Omega t) \tag{6}$$

where G is the gravitational constant, m_{sun} is the solar mass, $a \simeq 1\,\text{au}$ is the semi-major orbital axis, c is the speed of light, $\epsilon \simeq 0.0167$ is the orbital ellipticity, Ω is the earth's angular velocity, and k_α and k_μ are the freely floating parameters for the fit. The amplitude of annual variation is found to be $-1.9(3.0) \times 10^{-15}$. This can be combined with data from Hg$^+$ and the H-maser to place independent constraints of k_α and k_μ, as well as the coupling to the light quark mass k_q introduced by the H-maser. The combined data yields $k_\alpha = 2.5(3.1) \times 10^{-6}$, $k_\mu = -1.3(1.7) \times 10^{-5}$, and $k_q = -1.9(2.7) \times 10^{-5}$ [41].

4 Constraints of fundamental constant variation using molecular Sr$_2$

In the previous section, ultracold atomic Sr was used in a frequency measurement to exploit its (weak) α dependence. In contrast, ultracold molecular Sr$_2$ may be used for its μ dependence to constrain μ temporal drifts [14]. Molecules naturally exhibit spectral μ dependence since, in analogy to a mass on a spring, the ro-vibration of the constituent atoms (introducing m_p) is mediated through electronic interactions (introducing m_e).

Here, our interest turns to the bosonic strontium isotope, ^{88}Sr, whose lack of nuclear spin and hyperfine structure makes the molecular (and atomic) spectra much simpler. We have recently carried out narrow-line photoassociation studies with ^{88}Sr near the $^1S_0$-$^3P_1$ dissociation limit [15]. This was carried out in a state-insensitive lattice trap for the $^1S_0$-$^3P_1$ transition at 914 nm, permitting a recoil- and Doppler-free photoassociation process. The 15 kHz natural width of the molecular line can resolve every vibrational level near dissociation and has so far allowed observation of nine least-bound molecular states. The narrow molecular line shapes are sensitive to thermal effects even at 2 μK ultracold temperatures. One important feature of this narrow-line photoassociation is the large Franck-Condon overlap between the bound-state wave functions in the excited and ground electronic states. This overlap is predicted to lead to efficient production of ultracold ground-state molecules [15].

The proposed Sr$_2$ vibrational measurement is outlined in Fig. 6. Lattice-trapped ultracold ^{88}Sr atoms are associated by a two-color photoassociation process to $v' = -6$ and then $v = -3$ (v denotes vibrational quantum number in the ground potential X, v' denotes vibrational quantum number in the excited potential 0_u^+). This utilizes 689 nm laser light detuned from the $^1S_0$-$^3P_1$ atomic resonance. The vibrational quanta indicated are chosen to optimize cold molecule production efficiency. The next step is vibrational Raman spectroscopy $v = -3 \rightarrow v' \simeq 40 \rightarrow v = 27$. Here the $v = 27$ state is chosen because of its nearly maximal energy sensitivity
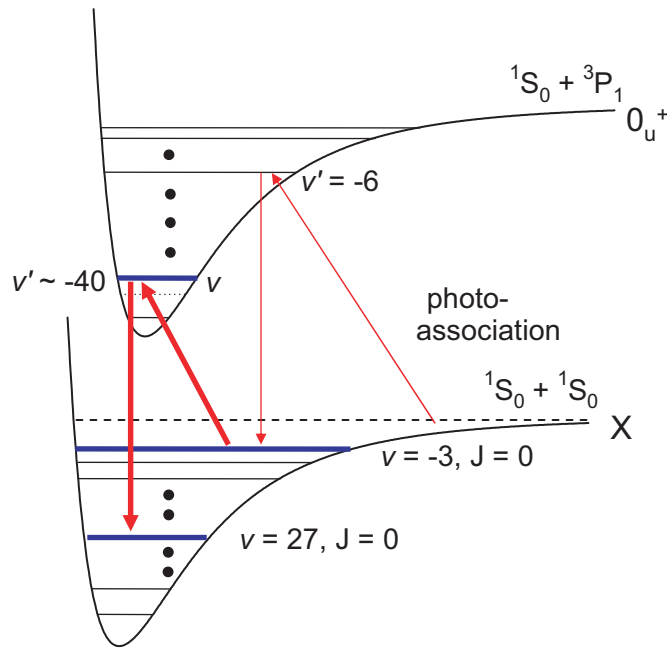
Fig. 6. Schematic of the proposed Sr_2 vibrational level Raman spectroscopy to constrain μ variation. Ultracold Sr atoms are first two-color photoassociated (thin arrows) to produce ultracold Sr_2 in the ground electronic state. Raman spectroscopy is then performed to measure the energy interval between vibrational states $v = -3$ and $v = 27$ (thick arrows). Note that positive vibrational quantum numbers count from the deeply bound potential minimum, whereas negative vibrational quantum numbers count from the dissociation limit.

to $\delta\mu/\mu$ [14]. The $v' = 40$ state is chosen to maximize the relevant dipole transition matrix elements. Subsequent measurements of the $v = -3$ to $v = 27$ energy interval separated by timescales of a year or so are estimated to help determine $\delta\mu/\mu$ at the 10^{-15}/yr level. This can be done with weak model dependence and does not rely on interpretation of the Schmidt model [42]. These measurements exploit the techniques of high measurement precision from the ^{87}Sr frequency standard, including laser stabilization, the frequency comb, lattice confinement with a zero-differential-AC-Stark shift, and ultranarrow spectra.

5 Conclusion

Considerable progress in the accuracy and stability of the Sr optical frequency standard makes this system well-suited to contribute to the measurement of changes in the fundamental constants. Both ultracold atomic ^{87}Sr and ultracold molecular ^{88}Sr$_2$ can play an important role in these measurements.

References

1. S.G. Karshenboim, V.V. Flambaum, E. Peik, *Handbook of Atomic, Molecular and Optical Physics* (Springer, 2005), p. 455
2. S.N. Lea, Rep. Prog. Phys. **70**, 1473 (2007)
3. V.V. Flambaum, M.G. Kozlov, Phys. Rev. Lett. **98**, 240801 (2007)
4. E. Reinhold, et al., Phys. Rev. Lett. **96**, 051101 (2006)
5. T.P. Heavner, S.R. Jefferts, E.A. Donley, J.H. Shirley, T.E. Parker, Metrologia **42**, 411 (2005)
6. S. Bize, et al., J. Phys. B **38**, S449 (2005)
7. E.J. Angstmann, V.A. Dzuba, V.V. Flambaum (2004) [`arXiv:physics/0407141v1`]
8. A.D. Ludlow, et al., Phys. Rev. Lett. **96**, 033003 (2006)
9. R. Le Targat, et al., Phys. Rev. Lett. **97**, 103003 (2006)
10. M. Takamoto, et al., J. Phys. Soc. Jpn. **75**, 104302 (2006)
11. M.M. Boyd, et al., Phys. Rev. Lett. **98**, 083002 (2007)
12. X. Baillard, et al., published online EpJD DOI: `10.1140/epjd/e2007-00330-3` (2007)
13. G.K. Campbell, et al. (in preparation)
14. T. Zelevinsky, S. Kotochigova, J. Ye, Phys. Rev. Lett. **100**, 043201 (2008)
15. T. Zelevinsky, et al., Phys. Rev. Lett. **96**, 203201 (2006)
16. P.G. Mickelson, et al., Phys. Rev. Lett. **95**, 223002 (2005)
17. A.D. Ludlow, et al., Science (accepted)
18. W.H. Oskay, et al., Phys. Rev. Lett. **97**, 020801 (2006)
19. H.S. Margolis, et al., Science **306**, 1355 (2004)
20. T. Schneider, E. Peik, C. Tamm, Phys. Rev. Lett. **94**, 230801 (2005)
21. Z.W. Barber, et al., Phys. Rev. Lett. **96**, 083002 (2006)
22. T. Rosenband, et al., Science (accepted)
23. M.M. Boyd, et al., Phys. Rev. A **76**, 022510 (2007)
24. H. Katori, et al., Phys. Rev. Lett. **91**, 173005 (2003)
25. T. Mukaiyama, et al., Phys. Rev. Lett. **90**, 113002 (2003)
26. T. Loftus, et al., Phys. Rev. Lett. **93**, 073003 (2004)
27. G. Wilpers, et al., Metrologia **44**, 146 (2007)
28. C. Degenhardt, et al., Phys. Rev. A **75**, 062111 (2005)
29. M. Takamoto, et al., Nature **435**, 321 (2005)
30. D. Leibfried, R. Blatt, C. Monroe, D. Wineland, Rev. Mod. Phys. **75**, 281 (2003)
31. H. Hachisu, et al., Phys. Rev. Lett. **100**, 053001 (2008)
32. R.W.P. Drever, et al., Appl. Phys. B **31**, 97 (1983)
33. M. Notcutt, et al., Opt. Lett. **30**, 1815 (2005)
34. A.D. Ludlow, et al., Opt. Lett. **32**, 641 (2007)
35. K. Numata, A. Kemery, J. Camp, Phys. Rev. Lett. **93**, 250602 (2004)
36. M.M. Boyd, et al., Science **314**, 1430 (2006)
37. S.M. Foreman, et al., Phys. Rev. Lett. **99**, 153601 (2007)
38. C.W. Oates, et al., IEEE Inter. Freq. Control Symposium Exposition, 74 (2006)
39. S.G. Porsev, A. Derevianko, Phys. Rev. A **74**, 020502R (2006)
40. S.M. Foreman, et al., Rev. Sci. Instrum. **78**, 021101 (2007)
41. S. Blatt, et al., Phys. Rev. Lett. (accepted)
42. V.V. Flambaum, A.F. Tedesco, Phys. Rev. C **73**, 055501 (2006)